

Journal of Materials Chemistry A

Accepted Manuscript



This is an *Accepted Manuscript*, which has been through the Royal Society of Chemistry peer review process and has been accepted for publication.

Accepted Manuscripts are published online shortly after acceptance, before technical editing, formatting and proof reading. Using this free service, authors can make their results available to the community, in citable form, before we publish the edited article. We will replace this *Accepted Manuscript* with the edited and formatted *Advance Article* as soon as it is available.

You can find more information about *Accepted Manuscripts* in the [Information for Authors](#).

Please note that technical editing may introduce minor changes to the text and/or graphics, which may alter content. The journal's standard [Terms & Conditions](#) and the [Ethical guidelines](#) still apply. In no event shall the Royal Society of Chemistry be held responsible for any errors or omissions in this *Accepted Manuscript* or any consequences arising from the use of any information it contains.



Journal Name

COMMUNICATION

Efficient adsorption of organic dyes on a flexible single-wall carbon nanotube film

Jian Luan, † Peng-Xiang Hou, † Chang Liu,* Chao Shi, Guo-Xian Li and Hui-Ming Cheng

Received 00th January 20xx,
Accepted 00th January 20xx

DOI: 10.1039/x0xx00000x

www.rsc.org/

A flexible single-wall carbon nanotube film prepared by simple filtration exhibited excellent adsorption of organic dyes under ultraviolet light in which a photodegradation-induced electrostatic interaction plays an important role.

Nowadays, a growing number of contaminants including heavy metals and dyes are detected in water, which poses a potential risk to human health and ecological systems.¹ Rhodamine B (RhB) is one of the most frequently used colorants in the textile and food industry. It is toxic and carcinogenic, and its biological degradation is very slow. At present, a number of methods such as photocatalytic degradation, sonochemical degradation, Fenton-based oxidation, and ozonation have been developed to remove RhB from waste water.² However, the selectivity of the above techniques is very poor, and the cost is high due to the fact that they cannot be reused. It is therefore important to find a more efficient way to selectively remove RhB.

Carbon materials, such as graphene,³ activated carbon,⁴ and carbon nanotubes (CNTs)⁵ with high surface area, good stability, and environmental friendly characteristics are considered to be ideal candidates for the adsorption of various heavy metal ions and organic pollutants.⁶ However, to the best of our knowledge, the reported RhB removal capability by now is still not satisfied (Table S1). In addition, it is worth noting that most of the developed adsorbents are powders, and this leads to serious recontamination and recycling problems. From this respect, a free-standing thin film or bulk materials are highly desired, but this usually comes with the problems of a reduction in both adsorption ability and stability in solutions.⁷ Therefore, to realize efficient, selective, and reversible RhB adsorption and desorption using a freestanding bulk material remains a big challenge.⁸

Here, a high purity, free-standing and robust single-wall carbon nanotube (SWCNT) film was fabricated by simple filtration of commercially available SWCNTs. The SWCNT film showed good flexibility, stiffness, and stability even in solutions. We explored this SWCNT film as a sorbent for the removal of RhB without involving any other complex process. The films showed excellent selective and repeatable adsorption and desorption for RhB with a record high adsorption of 190 mg g⁻¹ and a stability that showed no structure and performance degradation after 20 cycles under ultraviolet (UV) light irradiation.

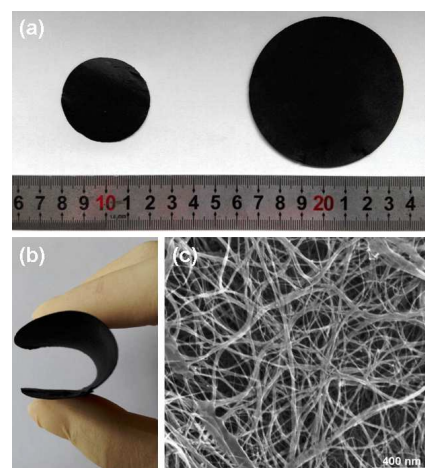


Fig. 1 (a and b) Optical images of SWCNT films of different sizes and excellent flexibility; (c) A typical SEM image of the SWCNT film.

The SWCNT films were fabricated by dispersing as-synthesized SWCNTs in a 0.5 wt% sodium dodecyl sulfate solution followed by filtration.⁹ The details of the origin of the SWCNTs and SWCNT film fabrication are given in the ESI. As shown in Figs. 1a and b, freestanding SWCNT films were obtained with tunable sizes, and showed excellent flexibility and processability. An SEM image (Fig. 1c) shows that the film is composed of entangled SWCNTs. The sheet resistance of the film was measured to be as low as 0.17 Ω sq⁻¹, much lower than the reported value of graphene paper.¹⁰ Interestingly, the SWCNT film has excellent structural stability, as

Shenyang National Laboratory for Materials Science, Institute of Metal Research, Chinese Academy of Sciences, Shenyang 110016, P. R. China. E-mail: cliu@imr.ac.cn; Fax: +86-24-23903126; Tel: +86-24-83978280

† Both authors contributed equally to the manuscript.

Electronic Supplementary Information (ESI) available: The additional information include: Sources of SWCNTs, characterization, flexible SWCNT film fabrication, HNO₃-doped flexible SWCNT film fabrication, the color change photograph image of dye solution, TGA, Raman, UV-vis spectra, and other related information. See DOI: 10.1039/x0xx00000x

evidenced by it retaining its intact film structure even under strong stirring conditions in both water and a RhB solution (Movies 1 and 2 in ESI).

The Brunauer–Emmett–Teller (BET) specific surface area and pore structure of the SWCNT film were characterized by nitrogen adsorption–desorption measurements. As shown in Fig. 2a, the isotherm shows adsorption throughout the whole relative pressure range, suggesting a wide pore size range and abundant pore. Analysis using the Barrett–Joyner–Halenda (BJH) equation shows that the mesopore sizes is mainly in the 2–10 nm range (inset in Fig. 2a). The BET surface area, micropore volume, mesopore volume and macropore volume were calculated to be $350 \text{ m}^2 \text{ g}^{-1}$, $0.2 \text{ cm}^3 \text{ g}^{-1}$, $0.25 \text{ cm}^3 \text{ g}^{-1}$, and $0.46 \text{ cm}^3 \text{ g}^{-1}$, respectively. Fig. 2b shows a TGA curve of a SWCNT film measured in a flow of air, and only one rapid oxidation peak at $784 \text{ }^\circ\text{C}$ is detected, suggesting the high quality and good uniformity of the SWCNTs. About 7% metal oxide residue was obtained, which corresponds to $\sim 5\%$ Fe catalyst impurity in the SWCNT film.

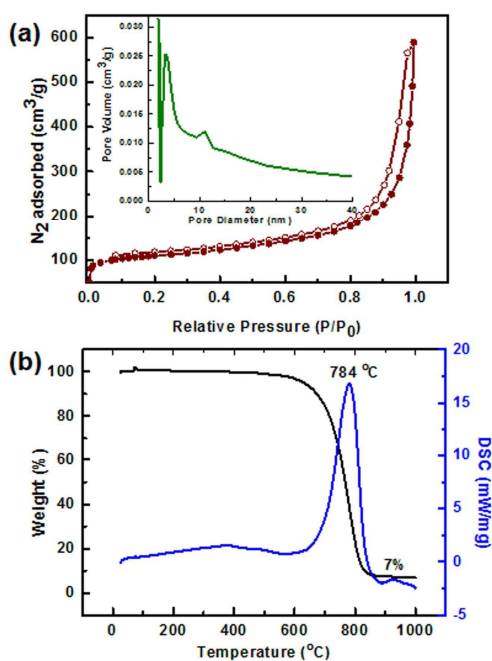


Fig. 2 (a) Nitrogen adsorption and desorption isotherms of a SWCNT film. The inset shows the pore size distribution; (b) TGA curve of a SWCNT film.

The adsorption behaviour of a SWCNT film was evaluated using RhB as a model adsorbate. Three other organic dyes including methylene blue (MB), methylene orange (MO) and congo red (CR) were used to evaluate the adsorption selectivity. The results of RhB (10 mg L^{-1}) adsorption monitored by UV–vis spectroscopy under UV light are shown in Fig. 3a. The adsorption amount of RhB reached 190 mg g^{-1} after 240 min under UV light irradiation, more than 1.3 times higher than the highest value reported for carbon materials (Fig. S3 and Table S1)⁸, where a Fe_3O_4 –graphene framework adsorbed 137 mg g^{-1} RhB⁸ⁱ. Parallel experiments under UV light without adding a SWCNT film (inset of Fig. 3a) and in the dark with a SWCNT film (Fig. S4a) were also performed for comparison. It was

found that only 34 mg g^{-1} RhB was removed after 240 min adsorption in the dark, and almost no RhB was adsorbed without the SWCNT film under UV light, suggesting that the SWCNT film is the key adsorbent although the UV light also plays an important role. Therefore, the adsorption of RhB by the SWCNT film is not a simple physical adsorption process, and photodegradation or light-related adsorption may be involved.

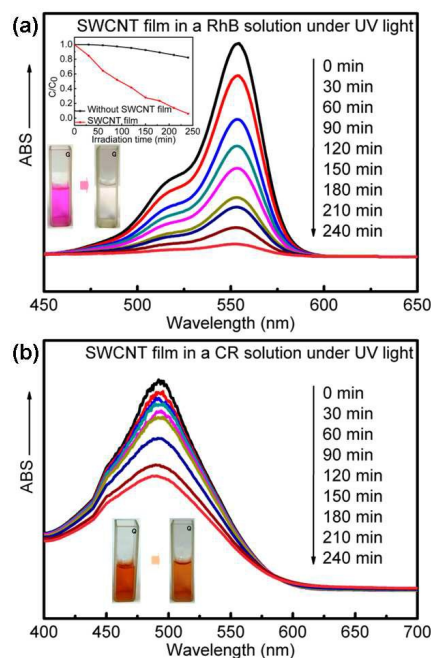


Fig. 3 UV-vis spectra of (a) RhB and (b) CR solutions after different adsorption times with the SWCNT film under UV light irradiation. Inset: decolorization rates and photographs of the (a) RhB and (b) CR solutions before and after adsorption. The initial concentrations of RhB and CR were 10 mg L^{-1} , the amount of SWCNT film adsorbent used was 5 mg.

The adsorption performance of a SWCNT film for CR under UV light is given in Figs. 3b and S4b, which show a low adsorption amount of 90 mg g^{-1} after 240 min. When the film was added to a mixture of RhB and CR, the RhB absorption peak decreased quickly, while the intensity of the characteristic CR absorption peak remained much higher (Fig. S5). The photographs in Fig. 4a show the gradual colour change of the mixed RhB and CR solution with prolonged adsorption time (up to 240 min). We can see that the removal of CR from the solution is not as apparent as for RhB. These results clearly show that the SWCNT film exhibits a superior adsorption capability towards RhB than to CR. This can be attributed to the different chemical compositions of these two dyes (Fig. S6). RhB has more positive functional groups, which may lead to efficient electrostatic adsorption. To verify this point, MB and MO were selected as adsorbates, because they have similar functional groups to RhB and CR. The adsorption amounts for MB and MO were measured to be 198 mg g^{-1} and 130 mg g^{-1} , respectively (Fig. S7), which verified that the adsorption capability is closely related to the chemical composition of the dyes. In addition, we compare the adsorption performance of our SWCNT films with other reported carbon-based adsorbents (Table S1), including Fe/ordered mesoporous carbon^{11a}, pinecone derived activated

carbon^{11b} and activated carbon fibers^{11c}. It can be seen that our SWCNT film shows a special-favored adsorption for RhB, demonstrating the highest adsorption ability.

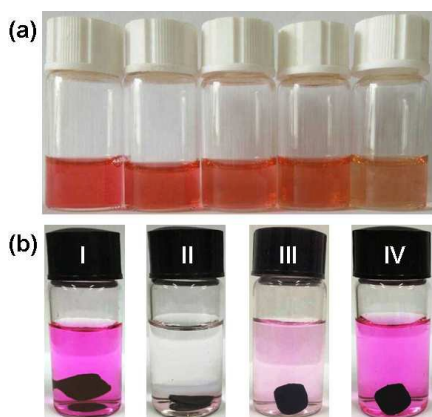
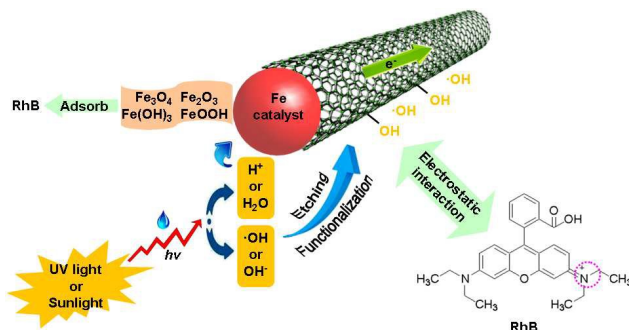


Fig. 4 (a) Photographs of a mixed RhB and CR solution upon SWCNT adsorption for different times; (b) Photographs showing the adsorption and desorption of RhB by the SWCNT film: (I) At the beginning of adsorption; (II) after 240 min adsorption; (III) after 2 h desorption; (IV) after 10 h desorption.

The cyclic adsorption/desorption performance of the SWCNT film was studied with a constant RhB concentration (10 mg L^{-1}) and amount of adsorbent (5 mg). After each cycle (240 min) of RhB adsorption, the SWCNT film was dipped into ethanol to desorb RhB. The amount of RhB in ethanol reached about 174 mg g^{-1} after 10 h (Fig. 4b). The residual unreleased RhB (16 mg g^{-1}) can be ascribed to chemical adsorption or photodegradation. The recovered SWCNT film was dried at $50 \text{ }^\circ\text{C}$ and reused for adsorption in the following cycles. There is no obvious adsorption decrease observed after 20 cycles (Fig. S8), indicating a reversible adsorption and desorption ability of the film. Furthermore, SEM observation shows that the structure of the film was well preserved after the adsorption-desorption cycles.

In order to understand the adsorption mechanism of the SWCNTs, we evaluated the adsorption capability of SWCNT films after HNO_3 purified treatment (denoted P-SWCNT), where residual Fe catalyst impurity was removed from the sample (Fig. S9). As shown in Fig. S10, the adsorption amount of RhB is about 174 mg g^{-1} , slightly lower than that of SWCNT films, while the same with the desorption amount of RhB for the SWCNT film. Therefore, it is reasonable to conclude that metal nanoparticles play a role in the photodegradation of RhB. It is well known that electrons can be captured from water molecules and oxygenated into $\bullet\text{OH}$ or OH^- active species under UV light. The $\bullet\text{OH}$ or OH^- radicals then functionalize the SWCNT surface to become negative, and to preferentially adsorb dye molecules with positive functional groups through electrostatic interaction. This is why higher RhB and MB adsorption amounts were obtained compared to MO and CR. At the same time, the reaction between Fe catalyst and H_2O or H^+ can generate passive iron oxides (Fe_3O_4 , Fe_2O_3 , $\text{Fe}(\text{OH})_3$, and FeOOH), which can also adsorb dye molecules.¹² A schematic showing the adsorption process of RhB on SWCNTs under UV light irradiation is given in Scheme 1.



Scheme 1 A schematic showing the adsorption process of RhB on SWCNTs under UV light irradiation.

To verify this proposed mechanism, we studied the adsorption performance of the SWCNT films under sunlight. As shown in Fig. S11, the adsorption ability under UV irradiation is higher than under visible irradiation (Scheme S1), which can be well understood considering that more photogenerated holes, electrons, $\bullet\text{OH}$ and OH^- radicals were produced under higher energy UV irradiation.¹³ This supports the proposed adsorption mechanism of photodegradation-induced electrostatic interaction.

In summary, we fabricated a freestanding, flexible SWCNT film by a simple filtration method. The SWCNT films had good processability and stability and exhibited excellent adsorption and desorption performance for organic dyes under UV light. Of particular note is that a RhB adsorption amount of 190 mg g^{-1} was achieved, which is more than 1.3 times higher than the highest value reported for carbon materials. In addition, the SWCNT films showed different adsorption ability toward organic dyes with different functional groups. We proposed a photodegradation-induced electrostatic interaction mechanism for the target dye adsorption characteristics. Our results open up possibilities for the use of macroscopic SWCNT films in water treatment.

This work is supported by the MOST of China (Grants 2011CB932601), NSFC (Grants 51102242, 51221264, 51272257), and Chinese Academy of Sciences (Grant KGZD-EW-T06).

Notes and references

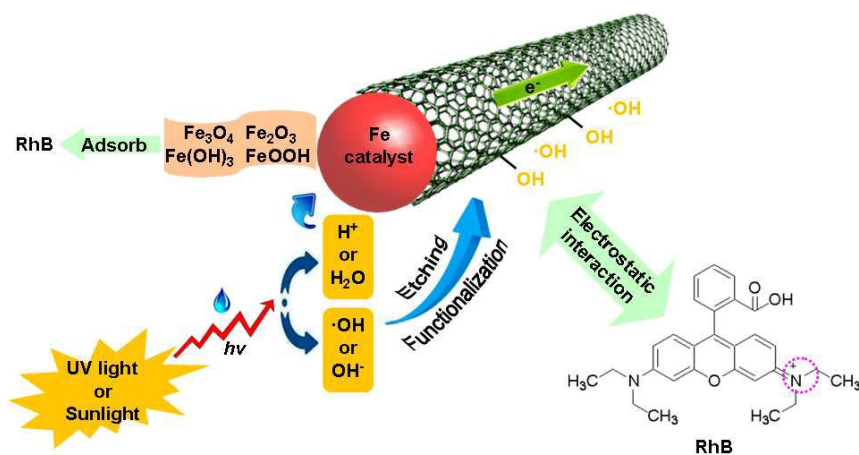
- (a) Y. F. Shen, *Renewable Sustainable Energy Rev.*, 2015, **43**, 281; (b) Z. G. Jia, L. L. Yang, J. H. Liu, Q. Z. Wang and R. S. Zhu, *J. Ind. Eng. Chem.*, 2015, **21**, 111; (c) H. Xu, C. S. Cao and B. Zhao, *Chem. Commun.*, 2015, **51**, 10280; (d) I. Ali, *Chem. Rev.*, 2012, **112**, 5073; (e) A. Adamczuk and D. Kołodyńska, *Chem. Eng. J.*, 2015, **274**, 200; (f) W. B. Wang, G. Y. Tian, Z. F. Zhang and A. Q. Wang, *Chem. Eng. J.*, 2015, **265**, 228; (g) M. Al-Shannag, Z. Al-Qodah, K. Bani-Melhem, M. R. Qtaishat and M. Alkasrawi, *Chem. Eng. J.*, 2015, **260**, 749. (h) L. X. Li, B. C. Li, L. Wu, X. Zhao and J. P. Zhang, *Chem. Commun.*, 2014, **50**, 7831; (i) Y. J. Ye, J. Chen, Q. Q. Ding, D. Y. Lin, R. L. Dong, L. B. Yang and J. H. Liu, *Nanoscale*, 2013, **5**, 5887.
- (a) Y. Li, X. F. Yin, F. R. Chen, H. H. Yang, Z. X. Zhuang and X. R. Wang, *Macromolecules*, 2006, **39**, 4497; (b) L. Zhu, T. Ghosh, C. Y. Park, Z. D. Meng, W. C. Oh, *Chin. J. Catal.*, 2012, **33**, 1276; (c) L. Zhang, Y. Nie, C. Hu, J. Qu, *Appl. Catal. B: Environ.*, 2012, **125**, 418; (d) T. Li, L. Zhao, Y. He, J. Cai, M. Luo, J. Lin, *Appl. Catal. B: Environ.*, 2013, **129**, 255.
- (a) A. K. Geim and K. S. Novoselov, *Nat. Mater.*, 2007, **6**, 183; (b) Y. B. Zhang, Y. W. Tan, H. L. Stormer and P. Kim, *Nature*,

- 2005, **438**, 201; (c) K. S. Novoselov, A. K. Geim, S. V. Morozov, D. Jiang, M. I. Katsnelson, I. V. Grigorieva, S. V. Dubonos and A. A. Firsov, *Nature*, 2005, **438**, 197; (d) K. S. Novoselov, A. K. Geim, S. V. Morozov, D. Jiang, Y. Zhang, S. V. Dubonos, I. V. Grigorieva and A. A. Firsov, *Science*, 2004, **306**, 666.
- 4 (a) R. Helleur, N. Popovic, M. Ikura, M. Stanciulescu, D. Liu, *J. Anal. Appl. Pyrol.*, 2001, **58–59**, 813; (c) J. L. Allen, J. L. Gatz and P. C. Eklund, *Carbon*, 1999, **37**, 1485; (c) T. A. Brady, M. Rostam-Abadi and M. J. Rood, *Gas Sep. Purif.*, 1996, **10**, 97; (b) M. Streat, J. W. Patrick and M. J. Camporro Perez, *Water Res.*, 1995, **29**, 467.
- 5 (a) M. F. L. De Volder, S. H. Tawfick, R. H. Baughman and A. J. Hart, *Science*, 2013, **339**, 535; (b) Q. Zhang, J. Q. Huang, W. Z. Qian, Y. Y. Zhang and F. Wei, *Small*, 2013, **9**, 1237; (c) M. Terrones, *Annu. Rev. Mater. Res.*, 2003, **33**, 419; (d) P. L. McEuen, M. S. Fuhrer and H. K. Park, *IEEE T. Nanotechnol.*, 2002, **1**, 78.
- 6 (a) C. Singh, S. Bansal, V. Kumar and S. Singhal, *Ceram. Int.*, 2015, **41**, 3595; (b) J. X. Xia, J. Di, S. Yin, H. M. Li, L. Xu, Y. G. Xu, C. Y. Zhang and H. M. Shu, *Ceram. Int.*, 2014, **40**, 4607; (c) D. A. Reddy, S. Lee, J. Choi, S. Park, R. Ma, H. Yang and T. K. Kim, *Appl. Surf. Sci.*, 2015, **341**, 175; (d) L. Sun, C. G. Tian, L. Wang, J. L. Zou, G. Mu and H. G. Fu, *J. Mater. Chem.*, 2011, **21**, 7232; (e) Y. H. Li, S. G. Wang, Z. K. Luan, J. Ding, C. L. Xu and D. H. Wu, *Carbon*, 2003, **41**, 1057; (f) Y. H. Li, Z. C. Di, J. Ding, D. H. Wu, Z. K. Luan and Y. Q. Zhu, *Water Res.*, 2005, **39**, 605; (g) S. H. Yang, W. H. Shin and J. K. Kang, *J. Chem. Phys.*, 2011, **134**, 244704; (h) C. Lu and H. Chiu, *Chem. Eng. Sci.*, 2006, **61**, 1138.
- 7 (a) P. M. Ajayan, *Chem. Rev.*, 1999, **99**, 1787; (b) F. Valentini, A. Amine, S. Orlanducci, M. L. Terranova and G. Palleschi, *Anal. Chem.*, 2003, **75**, 5413; (c) J. Wang, M. Musameh and Y. H. Lin, *J. Am. Chem. Soc.*, 2003, **125**, 2408; (d) J. Wang and M. Musameh, *Anal. Chem.*, 2003, **75**, 2075; (e) Z. H. Guo and S. J. Dong, *Anal. Chem.*, 2004, **76**, 2683.
- 8 (a) H. Xu, C. Wang, Y. H. Song, J. X. Zhu, Y. G. Xu, J. Yan, Y. X. Song and H. M. Li, *Chem. Eng. J.*, 2014, **241**, 35; (b) C. Singh, S. Bansal, V. Kumar and S. Singhal, *Ceram. Int.*, 2015, **41**, 3595; (c) Y. L. Xie, H. H. Qian, Y. J. Zhong, H. M. Guo and Y. Hu, *Int. J. Photoenergy*, 2012, **2012**, 682138; (d) C. Y. Yu, Y. R. Wang, Y. Liu, C. F. Guo and Y. Hu, *Mater. Lett.*, 2013, **100**, 278; (e) J. X. Xia, J. Di, S. Yin, H. M. Li, L. Xu, Y. G. Xu, C. Y. Zhang and H. M. Shu, *Ceram. Int.*, 2014, **40**, 4607; (f) J. P. Zhao, W. C. Ren and H. M. Cheng, *J. Mater. Chem.*, 2012, **22**, 20197; (g) L. Sun, C. G. Tian, L. Wang, J. L. Zou, G. Mu and H. G. Fu, *J. Mater. Chem.*, 2011, **21**, 7232; (h) Z. J. Huang, F. B. Li, B. F. Chen and G. Q. Yuan, *RSC Adv.*, 2015, **5**, 14027; (i) Y. M. Yang, G. W. Hu, F. J. Chen, J. Liu, W. S. Liu, H. L. Zhang and B. D. Wang, *Chem. Commun.*, 2015, **51**, 14405.
- 9 Z. C. Wu, Z. H. Chen, X. Du, J. M. Logan, J. Sippel, M. Nikolou, K. Kamaras, J. R. Reynolds, D. B. Tanner, A. F. Hebard and A. G. Rinzler, *Science*, 2004, **305**, 1273.
- 10 L. Paliotta, G. D. Bellis, A. Tamburrano, F. Marra, A. Rinaldi, S. K. Balijepalli, S. Kaciulis and M. S. Sarto, *Carbon*, 2015, **89**, 260.
- 11 (a) X. M. Peng, D. P. Huang, T. Odoom-Wubah, D. F. Fu, J. L. Huang and Q. D. Qin, *J. Colloid Interf. Sci.*, 2014, **430**, 272; (b) M. Samarghandi, M. Hadi, S. Moayedi and F. Askari, *Iran. J. Environ. Health Sci. Eng.*, 2009, **6**, 285; (c) C. Pelekani and V. L. Snoeyink, *Carbon*, 2001, **39**, 25.
- 12 (a) J. Fan, Y. H. Guo, J. J. Wang and M. H. Fan, *J. Hazard. Mater.*, 2009, **166**, 904; (b) R. A. Crane and T. B. Scott, *J. Hazard. Mater.*, 2012, **211–212**, 112.
- 13 R. Yuan, T. Chen, E. H. Fei, J. L. Lin, Z. X. Ding, J. L. Long, Z. Z. Zhang, X. Z. Fu, L. Wu and X. X. Wang, *ACS Catal.*, 2011, **1**, 200.

Efficient adsorption of organic dyes on a flexible single-wall carbon nanotube film

Jian Luan,[†] Peng-Xiang Hou,[†] Chang Liu,^{*} Chao Shi, Guo-Xian Li and Hui-Ming Cheng

A flexible single-wall carbon nanotube film prepared by simple filtration exhibited excellent adsorption of organic dyes under ultraviolet light in which a photodegradation-induced electrostatic interaction plays an important role.



* Corresponding author. Tel.: +86-24-83978280

E-mail address: cliu@imr.ac.cn (C. Liu)